

Four-weak-boson production at e^+e^- and pp supercolliders

V. Barger, T. Han, and H. Pi

Physics Department, University of Wisconsin, Madison, Wisconsin 53706

(Received 19 September 1989)

We evaluate the cross sections for $W^+W^-W^+W^-$ and $ZZZZ$ production in e^+e^- and pp collisions. For four- W production, the predicted cross section is 0.7–1.8 fb at a $\sqrt{s} = 2$ TeV e^+e^- collider, and 6–23 fb at the Superconducting Super Collider, depending on the Higgs-boson mass. The Higgs-boson contributions to four-weak-boson production processes are more significant than in the case of three-weak-boson production and would enhance the above cross sections by about a factor of 4 if $m_H \sim 0.3$ TeV.

I. INTRODUCTION

The production of two or more gauge bosons will be a major new area of study at future supercolliders.^{1–15} These processes are of great interest for several reasons. First, confirmation of tree-level predictions for the cross sections would provide stringent tests of the standard electroweak gauge model.^{1–5} The contributions of certain individual diagrams grow with energy and unitarity is satisfied through cancellations that require the precise gauge theory form of the interactions. Second, the ZZ , WW , and WWZ production processes are important in the search for a Higgs boson with mass $m_H > 2M_W$.^{6–10} Third, the study of weak-boson production will test the possibility that W bosons are strongly interacting or composite particles, since the predicted cross sections are then different from the standard-model results.¹¹ Even within the standard model, loop contributions associated with possible new heavy fermions can cause large deviations from tree-level cross-section predictions.¹² Fourth, the decays of possible gluinos, squarks, and new Z bosons to W and Z bosons provide important signatures for new particle searches^{13–15} and it is necessary to know the standard-model backgrounds to these and other similar new-physics signals.

The first tests of the predicted $WW\gamma$ and WWZ gauge couplings will likely be made with measurements of $ep \rightarrow eWX$ at DESY HERA,³ and $e^+e^- \rightarrow W^+W^-$ at CERN LEP II.⁴ Further studies of triple gauge couplings can be made with measurements of $W\gamma X$ and WZX production at the Fermilab Tevatron $p\bar{p}$ collider and at the pp colliders, the CERN Large Hadron Collider (LHC) and the Superconducting Super Collider (SSC).⁵ The $WWWW$, $WWZZ$, and $WWZ\gamma$ couplings enter significantly for the first time in the production of three gauge bosons. The cross sections for VVV production ($V = \gamma, W, \text{ or } Z$) have been recently evaluated^{8,9} using numerical calculations at the amplitude level in the helicity basis.¹⁶ At an e^+e^- supercollider with center-of-mass energy 0.5–2 TeV the VVV cross sections are 1–2 orders of magnitude below those for W^+W^- but still well within the range of observability;⁸ about 1000 events per

annum are predicted in each of the WWZ and $WW\gamma$ channels for an annual integrated luminosity of 10 fb^{-1} . The standard neutral Higgs boson H will appreciably enhance the WWZ event rate if its mass is in the range 0.2–0.6 GeV;^{8,9} the maximal enhancement is a factor of 1.4 for $m_H \sim 0.3$ GeV.

A natural extension of these standard-model calculations of multiple-gauge-boson production at future pp and e^+e^- supercolliders is the consideration of the production of four gauge bosons. Although we expect that these cross sections will be small, it is nonetheless interesting to investigate whether they might be observable. However, even with the numerical helicity amplitude methods, the calculation of four-gauge-boson production cross sections is still a formidable task because of the large number of Feynman graphs involved and multiple massive particles in the final state. Consequently, we restrict our present attention to an exploratory study of the two weak boson channels $W^+W^-W^+W^-$ ($4W$) and $ZZZZ$ ($4Z$) with fewest diagrams. Of the $VVVV$ cross sections with $V = W$ or Z we expect $4W$ to be the largest, $4Z$ to be the smallest, and mixed channels like $WWZZ$ to be intermediate, since the W coupling strength to fermions is stronger than the Z coupling strength.

We calculate the $4W$ and $4Z$ production cross sections in the standard model for e^+e^- and pp colliders versus the center of mass energy \sqrt{s} . At an e^+e^- collider with $\sqrt{s} = 2$ TeV and the SSC pp collider with $\sqrt{s} = 40$ TeV we obtain the following cross sections:

$$\begin{aligned}\sigma(e^+e^- \rightarrow 4W) &= 0.7 \text{ fb}, \\ \sigma(e^+e^- \rightarrow 4Z) &= 2.5 \times 10^{-3} \text{ fb},\end{aligned}\tag{1}$$

$$\sigma(pp \rightarrow 4WX) = 6 \text{ fb}, \quad \sigma(pp \rightarrow 4ZX) = 0.2 \text{ fb}.$$

Thus, with an integrated luminosity of 100 fb^{-1} , the expected numbers of $4W$ events would be

$$N(e^+e^- \rightarrow 4W) = 70 \text{ events},\tag{2}$$

$$N(pp \rightarrow 4WX) = 600 \text{ events},$$

before branching fractions to identifiable final states and acceptance efficiencies are imposed. With several years running at a high-luminosity 1–2-TeV machine the $e^+e^- \rightarrow 4W$ process might just be observable. The case for observing $pp \rightarrow 4WX$ is less certain because of QCD backgrounds and the smallness of the pure leptonic branching fraction of the W 's.

The above numbers assume that the Higgs-boson mass is either less than $2M_W$ or greater than 0.6 TeV. The above cross sections may be significantly enhanced if the Higgs boson has a mass in the 0.2–0.6-TeV range. For example with $m_H = 0.3$ TeV the $4W$ cross sections in Eq. (1) are increased by about a factor of 3 or 4. Any significant excess of the predicted rates would signal new physics beyond the standard model.

II. HELICITY AMPLITUDES

A. Feynman diagrams and notation

Figures 1 and 2 show the Feynman diagrams for $4Z$ and $4W$ production, respectively, in an R_ξ gauge. We work in the massless fermion approximation so diagrams with Higgs-boson couplings to fermions are not considered. The ϕ^\pm denote unphysical Higgs-boson exchanges which are absent in the unitary gauge. The physical Higgs boson H is present in several diagrams and enhances $4V$ production more than was the case for $3V$ production. We find important cancellations among the diagrams in these $4V$ production processes; hence measurements of the cross sections would stringently test the gauge couplings.

In the following we present the formulas for the helicity amplitudes of $4W$ and $4Z$ production. For clarity, we first introduce our conventions and notation and then give complete helicity amplitudes for the $f\bar{f} \rightarrow 4Z$ and $f\bar{f} \rightarrow 4W$ processes.

The couplings to fermions involve the quantities

$$g = (8M_W^2 G_F / \sqrt{2})^{1/2}, \quad g_Z = g / \cos \theta_W, \quad x_W = \sin^2 \theta_W, \quad (3)$$

$$g_\tau^f = g_V^f - \tau g_A^f, \quad g_V^f = \frac{1}{2}T_3 - Q_f x_W, \quad g_A^f = -\frac{1}{2}T_3,$$

where $\tau = \pm 1$ and Q_f and T_3 are the charge and the third component of weak isospin of fermion f . The propagator factors are

$$D_a(p_a) = \begin{cases} (p_H^2 - m_H^2 + im_H \Gamma_H)^{-1}, & a = H, \\ (p_\phi^2 - M_W^2 / \xi)^{-1}, & a = \phi \end{cases} \quad (4)$$

for scalar exchanges and

$$G_V^{\mu\nu}(p) = \begin{cases} g_{\mu\nu} / (p^2 + i\epsilon), & V = \gamma, \\ \frac{g_{\mu\nu} + (1 - \xi)p_\mu p_\nu / (\xi p^2 - M_V^2)}{p^2 - M_V^2 + iM_V \Gamma_V}, & \end{cases} \quad (5)$$

$$V = W^\pm, Z$$

for vector exchanges; here ξ is the gauge parameter with a value of 1 for Feynman gauge and 0 for unitary gauge. When a vector propagator is contracted with a four-vector X_ν the product will be denoted by

$$G_V^\mu(p, X) \equiv G_V^{\mu\nu}(p) X_\nu. \quad (6)$$

The triple-gauge-boson coupling is

$$T^{\lambda\mu\nu}(p_1, p_2) = (p_1 - p_2)^\lambda g^{\mu\nu} + (2p_2 + p_1)^\mu g^{\nu\lambda} - (2p_1 + p_2)^\nu g^{\lambda\mu}, \quad (7)$$

where p_1 and p_2 are four-momenta of bosons entering the triple vertex. The contraction of $T^{\lambda\mu\nu}$ with four-vectors X_μ and Y_ν will be denoted by

$$\Gamma^\lambda(p_1, p_2, X, Y) \equiv T^{\lambda\mu\nu}(p_1, p_2) X_\mu Y_\nu. \quad (8)$$

The quartic gauge-boson coupling is

$$S^{\mu\nu, \lambda\rho} = 2g^{\mu\nu} g^{\lambda\rho} - g^{\mu\lambda} g^{\nu\rho} - g^{\mu\rho} g^{\nu\lambda}. \quad (9)$$

The contraction of $S^{\mu\nu, \lambda\rho}$ with the four-vectors X_μ, Y_ν , and Z_ρ will be denoted by

$$L^\mu(X, Y, Z) \equiv S^{\mu\nu, \lambda\rho} X_\nu Y_\lambda Z_\rho. \quad (10)$$

The helicity amplitudes for the $4W$ and $4Z$ processes have the form

$$\mathcal{M}(\sigma_1 \sigma_2; \alpha_1 \alpha_2 \alpha_3 \alpha_4)$$

$$= i(4p_1^0 p_2^0)^{1/2} \chi_{-\sigma_2}^+(p_2) \mathcal{R}(\sigma_1 \sigma_2; \alpha_1 \alpha_2 \alpha_3 \alpha_4) \chi_{\sigma_1}(p_1), \quad (11)$$

where σ_1 (σ_2) labels the fermion (antifermion) helicities and $\alpha_1, \alpha_2, \alpha_3, \alpha_4$ denote the helicities of the weak bosons; p_1^0 and p_2^0 are the fermion energies. The explicit expressions for the helicity spinors $\chi_\sigma(p)$ with four-momenta p are given in Refs. 8 and 16. Following this formalism, the expressions for the reduced amplitudes \mathcal{R} are presented in terms of 2×2 matrices

$$[a_1, a_2, \dots, a_n]_\tau = (\not{a}_1)_\tau (\not{a}_2)_{-\tau} \dots (\not{a}_n)_{\delta_n \tau},$$

where $\delta_n = (-)^{n+1}$, $\tau = \pm 1$, and $(\not{a})_\pm = a_\mu \sigma_\pm^\mu$ with $\sigma_\pm^\mu = (\mathbf{1}, \pm \boldsymbol{\sigma})$. The $\boldsymbol{\sigma}$ are the Pauli matrices.

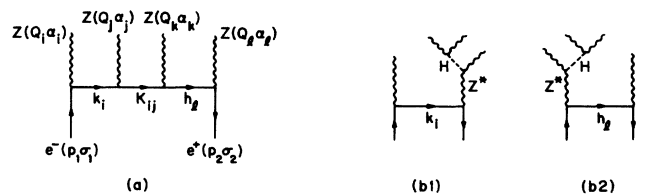


FIG. 1. Feynman diagrams for $e^+e^- \rightarrow ZZZZ$.

B. Amplitudes for $f\bar{f} \rightarrow ZZZZ$

The Feynman diagrams for the $4Z$ production process

$$e^-(p_1, \sigma_1) + e^+(p_2, \sigma_2) \rightarrow Z(Q_1, \alpha_1) + Z(Q_2, \alpha_2) \\ + Z(Q_3, \alpha_3) + Z(Q_4, \alpha_4) \quad (12)$$

are shown in Fig. 1. The reduced amplitude for Fig. 1(a) is

$$\mathcal{R}^{(a)}(\sigma_1\sigma_2; \alpha_1\alpha_2\alpha_3\alpha_4) \\ = g_Z^4 (g_{\sigma_2}^e)^4 \delta_{-\sigma_1\sigma_2} P[\epsilon_\ell h_\ell \epsilon_k K_{ij} \epsilon_j k_i \epsilon_i]_{\sigma_1} / (k_i^2 K_{ij}^2 h_\ell^2), \quad (13)$$

where P denotes a sum over the 24 permutations of the indices i, j, k, ℓ ; the ϵ 's are the polarization vectors of the outgoing Z 's and

$$k_i = p_1 - Q_i, \quad K_{ij} = k_i - Q_j, \quad h_\ell = Q_\ell - p_2. \quad (14)$$

The diagrams in Fig. 1(b) give the reduced amplitude

$$\mathcal{R}^{(b)} = -g_Z^4 M_Z^2 (g_{\sigma_2}^e)^2 \delta_{-\sigma_1\sigma_2} \sum_{i,\ell(i \neq \ell)}^4 (A^{(b1)} + A^{(b2)}), \quad (15)$$

where

$$A^{(b1)} = D_H(p_H)(\epsilon_j \cdot \epsilon_k) [G_Z(p_Z, \epsilon_\ell) k_i \epsilon_i]_{\sigma_1} / k_i^2, \quad (16)$$

$$A^{(b2)} = D_H(p_H)(\epsilon_j \cdot \epsilon_k) [\epsilon_\ell h_\ell G_Z(p'_Z, \epsilon_i)]_{\sigma_1} / h_\ell^2.$$

Here p_H , p_Z , and p'_Z are the momenta of the Higgs boson and the virtual Z , respectively:

$$p_H = Q_j + Q_k, \quad p_Z = p_2 + k_i, \quad p'_Z = p_1 - h_\ell, \quad (17)$$

and the four-vector G_Z is defined in Eq. (6). Note that the values of indices j and k are fixed once the values of i and ℓ are given by the summation in Eq. (15).

The reduced amplitudes for

$$q(p_1, \sigma_1) + \bar{q}(p_2, \sigma_2) \rightarrow Z(Q_1, \alpha_1) + Z(Q_2, \alpha_2) \\ + Z(Q_3, \alpha_3) + Z(Q_4, \alpha_4), \quad (18)$$

with massless quarks, are obtained by replacing the coupling $g_{\sigma_2}^e$ by $g_{\sigma_2}^q$ in Eqs. (13)–(17).

C. Amplitudes for $f\bar{f} \rightarrow W^+W^-W^+W^-$

The Feynman diagrams for the $4W$ production process

$$e^-(p_1, \sigma_1) + e^+(p_2, \sigma_2) \rightarrow W^-(q_1, \alpha_1) + W^+(Q_1, \beta_1) \\ + W^-(q_2, \alpha_2) + W^+(Q_2, \beta_2) \quad (19)$$

are shown in Fig. 2. Throughout this section, we will use the following notation in the reduced amplitudes:

$$k_i = p_1 - q_i, \quad K_{ij} = k_i - Q_j, \quad h_{j'} = Q_{j'} - p_2, \quad (20)$$

$$i' = 3 - i, \quad j' = 3 - j;$$

$$p_{V_1} = p_1 + p_2, \quad p_V = q_i + Q_j, \quad p'_{V'} = q_{i'} + Q_{j'}, \quad (21)$$

$$p_W = p_{V_1} - q_i, \quad p'_{W'} = p_{V_1} - Q_{j'};$$

$$J_V^\mu = G_V^\mu(p_V, \Gamma(-Q_j, -q_i, \epsilon_j, \epsilon_i)), \quad (22)$$

$$J'_{V'}^\mu = G_{V'}^\mu(p'_{V'}, \Gamma(-Q_{j'}, -q_{i'}, \epsilon_{j'}, \epsilon_{i'})).$$

The reduced amplitude for Fig. 2(a) is

$$\mathcal{R}^{(a)}(\sigma_1\sigma_2; \alpha_1\beta_1\alpha_2\beta_2) \\ = \frac{1}{4} g^4 \delta_{-1\sigma_1} \delta_{1\sigma_2} \sum_{i,j=1}^2 \frac{[\epsilon_{j'} h_{j'} \epsilon_{i'} K_{ij} \epsilon_j k_i \epsilon_i]_{\sigma_1}}{k_i^2 K_{ij}^2 h_{j'}^2}. \quad (23)$$

The reduced amplitudes for the other diagrams are as follows For Fig. 2(b),

$$\mathcal{R}^{(b)} = -\frac{1}{2} g^4 \delta_{-1\sigma_1} \delta_{1\sigma_2} \\ \times \sum_{V=\gamma,Z} \sum_{i,j=1}^2 (Q_e x_W)^{1-\delta_{VZ}} (g_+^e)^{\delta_{VZ}} \\ \times (A^{(b1)} + A^{(b2)} + \delta_{VZ} A^{(b3)}), \quad (24)$$

with δ_{VZ} the Kronecker delta ($\delta_{VZ} = 1$ for $V = Z$ and $\delta_{VZ} = 0$ for $V = \gamma$) and

$$A^{(b1)} = \frac{[J_V^\mu K_{ij} \epsilon_j k_i \epsilon_i]_{\sigma_1}}{k_i^2 K_{ij}^2}, \\ A^{(b2)} = \frac{[\epsilon_{j'} h_{j'} \epsilon_{i'} K_{ij} J_V]_{\sigma_1}}{K_{ij}^2 h_{j'}^2}, \quad (25)$$

$$A^{(b3)} = \frac{[\epsilon_{j'} h_{j'} F_{(b3)} k_i \epsilon_i]_{\sigma_1}}{k_i^2 h_{j'}^2},$$

$$F_{(b3)}^\mu = G_V^\mu(q_{i'} + Q_j, \Gamma(-Q_j, -q_{i'}, \epsilon_j, \epsilon_{i'})).$$

For Fig. 2(c),

$$\begin{aligned} \mathcal{R}^{(c)} &= g^4 x_W^2 \delta_{-\sigma_1 \sigma_2} \\ &\times \sum_{V_1, V_2 = \gamma, Z} \sum_{i, j = 1}^2 Q_e^{\delta_{V_1 \gamma} + \delta_{V_2 \gamma}} \left(\frac{g_{\sigma_2}^e}{x_W} \right)^{\delta_{V_1 Z} + \delta_{V_2 Z}} \\ &\times \frac{[J'_{V_2} K_{ij} J_{V_1}]_{\sigma_1}}{K_{ij}^2}. \end{aligned} \quad (26)$$

For Fig. 2(d),

$$\begin{aligned} \mathcal{R}^{(d)} &= \frac{1}{2} g^4 \delta_{-1 \sigma_1} \delta_{1 \sigma_2} \sum_{V = \gamma, Z} \sum_{i, j = 1}^2 (x_W)^{\delta_{V \gamma}} (1 - x_W)^{\delta_{V Z}} \\ &\times (A^{(d1)} + A^{(d2)}) \end{aligned} \quad (27)$$

with

$$A^{(d1)} = [F_{(d1)} k_i \epsilon_i]_{\sigma_1} / k_i^2,$$

$$F_{(d1)}^\mu = G_W^\mu(p_W, -\Gamma(p'_V, Q_j, J'_V, \epsilon_j)),$$

$$A^{(d2)} = [\epsilon_j h_j F_{(d2)}]_{\sigma_1} / h_j^2,$$

$$F_{(d2)}^\mu = G_W^\mu(p'_W, \Gamma(p_V, q_j, J_V, \epsilon_j)).$$

For Fig. 2(e), involving Higgs-boson exchange,

$$\mathcal{R}^{(e)} = -\frac{1}{2} g^4 M_W^2 \delta_{-1 \sigma_1} \delta_{1 \sigma_2} \sum_{i, j = 1}^2 (A^{(e1)} + A^{(e2)}), \quad (29)$$

with

$$A^{(e1)} = D_H(p'_V) \epsilon_i \cdot \epsilon_j [F_{(e1)} k_i \epsilon_i]_{\sigma_1} / k_i^2,$$

$$F_{(e1)}^\mu = G_W^\mu(p_W, \epsilon_j),$$

$$A^{(e2)} = D_H(p_V) \epsilon_i \cdot \epsilon_j [\epsilon_j h_j F_{(e2)}]_{\sigma_1} / h_j^2,$$

$$F_{(e2)}^\mu = G_W^\mu(p'_W, \epsilon_j).$$

(30)

(28) For Fig. 2(f),

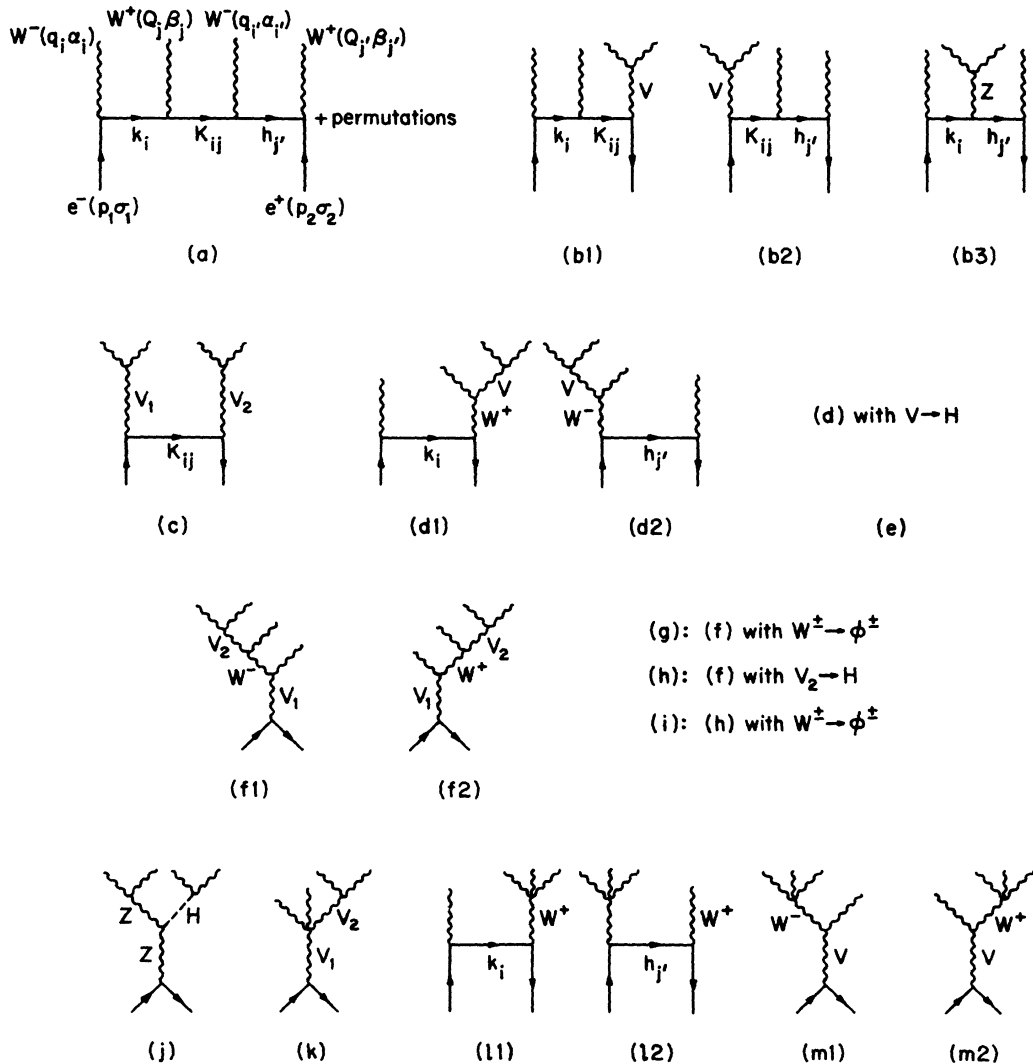


FIG. 2. Feynman diagrams for $e^+e^- \rightarrow W^-W^+W^-W^+$ in R_ξ gauge.

$$\mathcal{R}^{(f)} = -g^4 \delta_{-\sigma_1 \sigma_2} \sum_{V_1, V_2 = \gamma, Z} \sum_{i, j=1}^2 Q_e^{\delta_{V_1 \gamma}} (g_{\sigma_2}^e)^{\delta_{V_1 Z}} x_W^{\delta_{V_1 \gamma} + \delta_{V_2 \gamma}} (1 - x_W)^{\delta_{V_2 Z}} ([F_{(f1)}]_{\sigma_1} + [F_{(f2)}]_{\sigma_1}) \quad (31)$$

with

$$F_{(f1)}^\mu = G_{V_1}^\mu(p_{V_1}, \Gamma(-Q_{j'}, -p'_W, \epsilon_{j'}, T_1)), \quad F_{(f2)}^\mu = G_{V_1}^\mu(p_{V_1}, \Gamma(-p_W, -q_i, T_2, \epsilon_i)),$$

given in terms of

$$T_1^\mu = G_W^\mu(p'_W, \Gamma(p_V, q_{i'}, J_{V_2}, \epsilon_{i'})), \quad T_2^\mu = G_W^\mu(p_W, -\Gamma(p'_V, Q_j, J'_{V_2}, \epsilon_j)). \quad (32)$$

In Fig. 2(g), involving unphysical scalar exchanges, the reduced amplitude is

$$\mathcal{R}^{(g)} = -g^4 M_W^2 x_W^2 \delta_{-\sigma_1 \sigma_2} \sum_{V_1, V_2 = \gamma, Z} \sum_{i, j=1}^2 \frac{(-1)^{\delta_{V_2 Z}} (-Q_e)^{\delta_{V_1 \gamma}}}{(1 - x_W)^{\delta_{V_1 Z}}} (g_{\sigma_2}^e)^{\delta_{V_1 Z}} (A^{(g1)} + A^{(g2)}) \quad (33)$$

with

$$A^{(g1)} = D_\phi(p_V) \epsilon_i \cdot J_{V_2} [G_{V_1}(p_{V_1}, \epsilon_{j'})]_{\sigma_1}, \quad A^{(g2)} = D_\phi(p'_V) \epsilon_j \cdot J'_{V_2} [G_{V_1}(p_{V_1}, \epsilon_i)]_{\sigma_1}. \quad (34)$$

In the limit $\xi \rightarrow 0$, $D_\phi \rightarrow 0$, these contributions vanish.

The graphs in Fig. 2(h) give

$$\mathcal{R}^{(h)} = g^4 M_W^2 \delta_{-\sigma_1 \sigma_2} \sum_{V = \gamma, Z} \sum_{i, j=1}^2 (Q_e x_W)^{\delta_{V \gamma}} (g_{\sigma_2}^e)^{\delta_{V Z}} (A^{(h1)} + A^{(h2)}), \quad (35)$$

where

$$A^{(h1)} = D_H(p_V) \epsilon_i \cdot \epsilon_j [G_V(p_{V_1}, \Gamma(-Q_{j'}, -p'_W, \epsilon_{j'}, T))]_{\sigma_1}, \quad (36)$$

$$A^{(h2)} = D_H(p'_V) \epsilon_{i'} \cdot \epsilon_{j'} [G_V(p_{V_1}, \Gamma(-p_W, -q_i, T', \epsilon_i))]_{\sigma_1},$$

with

$$T^\mu = G_W^\mu(p'_W, \epsilon_{i'}), \quad T'^\mu = G_W^\mu(p_W, \epsilon_j).$$

Similarly, for Fig. 2(i),

$$\mathcal{R}^{(i)} = -\frac{1}{2} g^4 M_W^2 x_W \delta_{-\sigma_1 \sigma_2} \sum_{V = \gamma, Z} \sum_{i, j=1}^2 \frac{(-Q_e)^{\delta_{V \gamma}}}{(1 - x_W)^{\delta_{V Z}}} (g_{\sigma_2}^e)^{\delta_{V Z}} (A^{(i1)} + A^{(i2)}), \quad (37)$$

where

$$A^{(i1)} = D_\phi(p'_W) D_H(p_V) \epsilon_i \cdot \epsilon_j \epsilon_{i'} \cdot (p_V + p'_W) [G_V(p_{V_1}, \epsilon_{j'})]_{\sigma_1}, \quad (38)$$

$$A^{(i2)} = D_\phi(p_W) D_H(p'_V) \epsilon_{i'} \cdot \epsilon_{j'} \epsilon_j \cdot (p'_V + p_W) [G_V(p_{V_1}, \epsilon_i)]_{\sigma_1}.$$

These contributions also vanish in the unitary gauge.

For Fig. 2(j), the result is

$$\mathcal{R}^{(j)} = g^4 M_W^2 g_{\sigma_2}^e / (1 - x_W) \delta_{-\sigma_1 \sigma_2} \sum_{i, j=1}^2 D_H(p'_V) \epsilon_{i'} \cdot \epsilon_{j'} [G_Z(p_{V_1}, J_Z)]_{\sigma_1}. \quad (39)$$

The diagram of Fig. 2(k) involving the quartic gauge-boson coupling gives

$$\mathcal{R}^{(k)} = g^4 \delta_{-\sigma_1 \sigma_2} \sum_{V_1, V_2 = \gamma, Z} \sum_{i, j=1}^2 (Q_e)^{\delta_{V_1 \gamma}} (g_{\sigma_2}^e)^{\delta_{V_1 Z}} x_W^{\delta_{V_1 \gamma} + \delta_{V_2 \gamma}} (1 - x_W)^{\delta_{V_2 Z}} [G_{V_1}(p_{V_1}, T)]_{\sigma_1}, \quad (40)$$

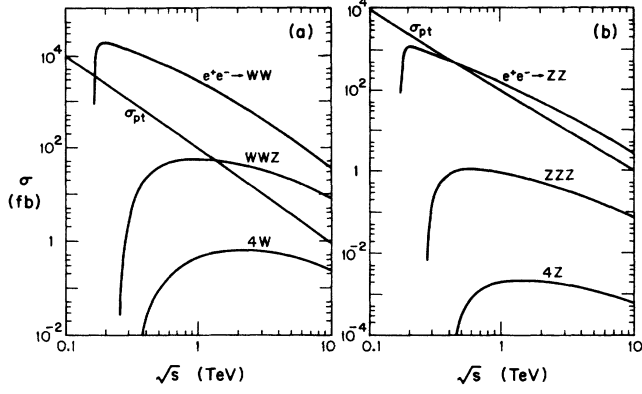


FIG. 3. Energy dependence of total cross sections for the processes (a) $e^+e^- \rightarrow W^+W^-$, W^+W^-Z , and $4W$; (b) $e^+e^- \rightarrow ZZ$, ZZZ , and $4Z$; with no significant Higgs-boson contributions ($m_H \lesssim 0.1$ TeV, or $m_H \gtrsim 0.6$ TeV). As a comparison, $\sigma_{pt} = 4\pi\alpha^2/3s$ is also illustrated.

where

$$T^\mu = L^\mu(J'_{V_2}, \epsilon_i, \epsilon_j).$$

For Fig. 2(l) the reduced amplitude is

$$\mathcal{R}^{(l)} = \frac{1}{2}g^4\delta_{-1\sigma_1}\delta_{1\sigma_2} \sum_{i,j=1}^2 (A^{(l1)} + A^{(l2)}) \quad (41)$$

where

$$A^{(l1)} = [Tk_i\epsilon_i]_{\sigma_1}/k_i^2,$$

$$T^\mu = G_W^\mu(p_W, L(\epsilon_{i'}, \epsilon_j, \epsilon_{j'})),$$

(42)

$$A^{(l2)} = [\epsilon_j h_j T']_{\sigma_1}/h_j^2,$$

$$T'^\mu = G_W^\mu(p'_W, L(\epsilon_j, \epsilon_i, \epsilon_{i'})).$$

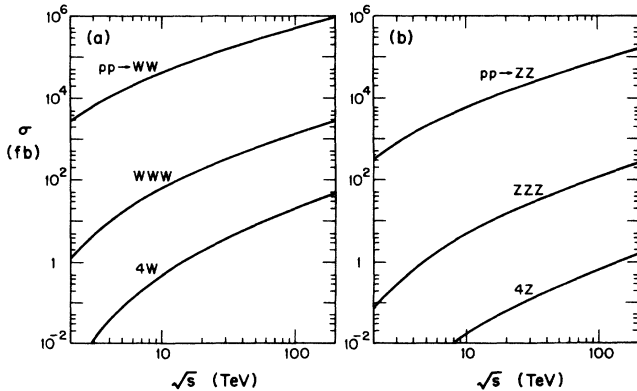


FIG. 4. Energy dependence of total cross sections of the processes (a) $pp \rightarrow W^+W^-$, WWW ($W^+W^+W^- + W^+W^-W^-$), and $4W$ ($W^+W^-W^+W^-$); (b) $pp \rightarrow ZZ$, ZZZ , and $4Z$; with no significant Higgs-boson contributions ($m_H \lesssim 0.1$ TeV or $m_H \gtrsim 0.6$ TeV).

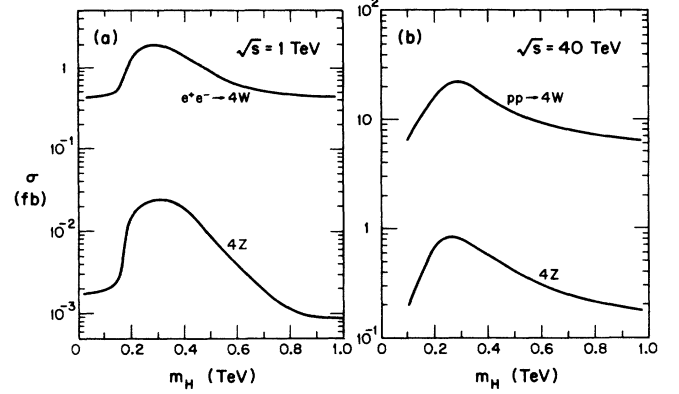


FIG. 5. Total cross sections versus m_H for the processes (a) $e^+e^- \rightarrow 4W$ and $4Z$ at $\sqrt{s} = 1$ TeV; (b) $pp \rightarrow 4W$ and $4Z$ at $\sqrt{s} = 40$ TeV.

Finally, for Fig. 2(m),

$$\mathcal{R}^{(m)} = -g^4\delta_{-\sigma_1\sigma_2} \sum_{V=\gamma,Z} \sum_{i,j=1}^2 (Q_e x_W)^{\delta_{V\gamma}} (g_{\sigma_2}^e)^{\delta_{VZ}} \times (A^{(m1)} + A^{(m2)}), \quad (43)$$

where

$$A^{(m1)} = [G_V(p_{V_1}, \Gamma(-Q_{j'}, -p'_W, \epsilon_{j'}, T))]_{\sigma_1},$$

$$T^\mu = G_W^\mu(p'_W, L(\epsilon_j, \epsilon_i, \epsilon_{i'})),$$

(44)

$$A^{(m2)} = [G_V(p_{V_1}, \Gamma(-p_W, -q_i, T', \epsilon_i))]_{\sigma_1},$$

$$T'^\mu = G_W^\mu(p_W, L(\epsilon_{i'}, \epsilon_j, \epsilon_{j'})).$$

The reduced amplitudes for $q\bar{q} \rightarrow 4W$ can be obtained from the preceding formulas for $e^+e^- \rightarrow 4W$ by (i) re-

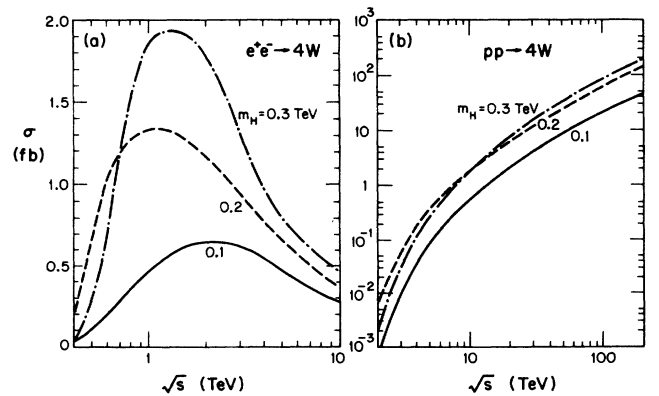


FIG. 6. Energy dependence of total cross sections for three values of the Higgs-boson mass $m_H = 0.1, 0.2,$ and 0.3 TeV for the processes (a) $e^+e^- \rightarrow 4W$; (b) $pp \rightarrow 4W$.

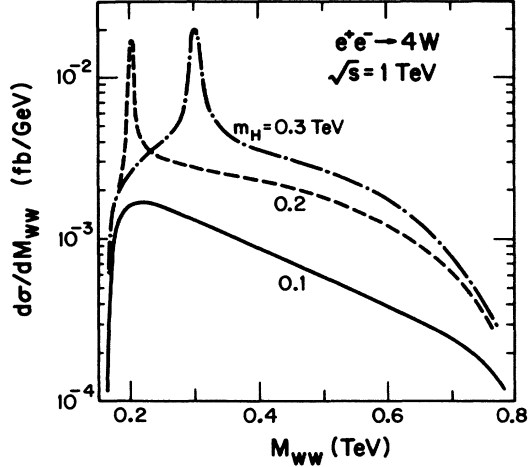


FIG. 7. W^+W^- pair invariant-mass distribution for $e^+e^- \rightarrow 4W$ at $\sqrt{s} = 1$ TeV for $m_H = 0.1, 0.2,$ and 0.3 TeV.

placing Q_e by Q_q and g_e^e by g_q^e , (ii) dropping the δ_{VZ} factor multiplying $A^{(b3)}$ in Eq. (24), and (iii) interchanging $W^-(q_i, \alpha_i)$ and $W^+(Q_i, \beta_i)$ for the $u\bar{u} \rightarrow 4W$ process.

III. CROSS SECTIONS AND DISTRIBUTIONS

The matrix elements presented in the previous section are in an arbitrary R_ξ gauge. We have checked that our calculated cross sections are independent of the gauge parameter ξ , which is a direct test of gauge invariance of the matrix elements. We also checked the Lorentz invariance of the calculated cross sections.

Using the formulas in Sec. II we have calculated the integrated cross sections for $4W$ and $4Z$ production at e^+e^- and pp colliders versus the total c.m. energy \sqrt{s} . The results are given in Figs. 3 and 4 for the case that $m_H < 2M_W$. For comparison, the cross sections for pair and triple-gauge-boson production are also shown. At energies above the threshold region, the $4W$ cross sections are suppressed by about 2 orders of magnitude relative to the WWZ and the $3W$ ($W^+W^+W^- + W^+W^-W^-$) cross sections. In e^+e^- collisions, the $4W$ and $4Z$ cross sections are rather flat over the region of $\sqrt{s} \sim 0.8$ – 10 TeV, and the maximum values occur at a c.m. energy of about 2 TeV, which is the proposed energy for the CLIC machine at CERN. The cross sections in pp collisions increase monotonically with increasing \sqrt{s} due to the larger parton luminosity at higher energies.

A standard-model neutral Higgs boson will enhance the cross sections for $4W$ and $4Z$ production if its mass is in the range $2M_W \lesssim m_H \lesssim 0.8$ TeV. Figure 5 shows the change in the cross sections with m_H for e^+e^- collisions at $\sqrt{s} = 1$ TeV and pp collisions at $\sqrt{s} = 40$ TeV. The $e^+e^- \rightarrow 4W$ cross section is enhanced by a factor of about 4 for $m_H \sim 0.3$ TeV. Figure 6 gives the e^+e^- and pp cross sections versus the c.m. energy \sqrt{s} for the three values $m_H = 0.1, 0.2, 0.3$ TeV of the Higgs-boson mass. The presence of the Higgs boson gives peaks in the

distribution of W^+W^- invariant mass at m_H as shown in Fig. 7, which is averaged over all W^+W^- combinations in $e^+e^- \rightarrow 4W$ events at $\sqrt{s} = 1$ TeV.

The W bosons produced in e^+e^- collisions may be identified by leptonic or hadronic decay modes. For $m_t > M_W$, the W branching fractions are

$$B(W \rightarrow \ell\nu) = 21.6\%,$$

$$B(W \rightarrow \tau\nu) = 10.8\%,$$

$$B(W \rightarrow q\bar{q}') = 67.6\%,$$

where ℓ is a charged lepton (e or μ); q, \bar{q}' are quarks (u, d, c, s, b) which will lead primarily to two jets that reconstruct the mass of the parent W . The τ may be identified in its decays to hadron jets (with low multiplicity and low invariant mass). The combined branching fractions for some of the final states from $e^+e^- \rightarrow 4W$ production are

$$B(8 \text{ jets}) \simeq 0.20,$$

$$B(1\ell, \not{p}_T, 6 \text{ jets}) \simeq 0.27,$$

$$B(\ell^+\ell^-, \not{p}_T, 4 \text{ jets}) \simeq 0.09,$$

$$B(\ell^\pm\ell^\pm, \not{p}_T, 4 \text{ jets}) \simeq 0.04,$$

$$B(\ell^\pm\ell^\pm\ell^\mp, \not{p}_T, 2 \text{ jets}) \simeq 0.03,$$

$$B(4\ell^\pm, \not{p}_T) \simeq 0.002,$$

where \not{p}_T denotes missing transverse momentum.

The reconstruction of $4W$ events is a complex problem depending on separation and pairing of jets, beam-pipe losses, \not{p}_T resolution, etc. These issues have been considered in Ref. 8 for the case of $e^+e^- \rightarrow WWZ$ production; in that case an acceptance factor of 70% (50%) at $\sqrt{s} = 1$ TeV (2 TeV) was estimated from typical separation requirements and beam-pipe losses.

If we assume a branching fraction of order 50% for identifiable $e^+e^- \rightarrow 4W$ events and an acceptance factor of order 50% (30%) at $\sqrt{s} = 1$ TeV (2 TeV), then the signal would be only 10 events for an integrated luminosity of 100 fb^{-1} . For a Higgs-boson mass $m_H \simeq 0.3$ TeV, this event rate would be a factor of 4 higher. Any significant excess above these predicted rates would indicate new physics beyond the standard model.

The reconstruction of $4W$ events at hadron colliders

may be problematic. Because of the large QCD backgrounds it may be difficult to identify the hadronic decay modes of W bosons (e.g., $\ell^\pm \ell^\pm \ell^\mp + \cancel{p}_T + 2$ jets events from $4W$ production could have a background from $3W+2$ QCD jets with $M_{jj} \simeq M_W$) and the branching fraction for all $4W$ bosons to decay leptonically is very small.

ACKNOWLEDGMENTS

This research was supported in part by the University of Wisconsin Research Committee with funds granted by the Wisconsin Alumni Research Foundation, and in part by the U.S. Department of Energy under Contract No. DE-AC02-76ER00881.

-
- ¹R. W. Brown and K. O. Mikaelian, Phys. Rev. D **19**, 922 (1979); R. W. Brown, D. Sahdev, and K. O. Mikaelian, *ibid.* **20**, 1164 (1979); D. A. Dicus and R. Vega, Phys. Rev. Lett. **57**, 1110 (1986); J. F. Gunion and A. Tofight-Niaki, *ibid.* **57**, 2351 (1986); A. Abbasabadi, W. W. Repko, D. A. Dicus, and R. Vega, Phys. Rev. D **38**, 2770 (1988); C. Ahn *et al.*, SLAC Report No. 329, 1988 (unpublished); M. E. Peskin, Report No. SLAC-PUB-4601, 1988 (unpublished); K. J. F. Gaemers and M. R. van Velzen, Z. Phys. C **43**, 103 (1989).
- ²E. Eichten, I. Hinchliffe, K. Lane, and C. Quigg, Rev. Mod. Phys. **56**, 579 (1984); **58**, 1065(E) (1986).
- ³E. Gabrielli, Mod. Phys. Lett. A **1**, 465 (1986); U. Baur and D. Zeppenfeld, Report No. CERN-TH-5362, 1989 (unpublished), and references therein.
- ⁴K. Hagiwara, R. D. Peccei, D. Zeppenfeld, and K. Hikasa, Nucl. Phys. **B282**, 253 (1987).
- ⁵D. Zeppenfeld and S. Willenbrock, Phys. Rev. D **37**, 1775 (1988); U. Baur and D. Zeppenfeld, Nucl. Phys. **B308**, 127 (1988).
- ⁶For recent reviews of Higgs-boson search via ZZ , WW decay modes, see, e.g., R. N. Cahn *et al.*, in *Experiments, Detectors, and Experimental Areas for the Supercollider*, proceedings of the Workshop, Berkeley, California, 1987, edited by R. Donaldson and M. Gilchriese (World Scientific, Singapore, 1988), p. 20; V. Barger, in *Proceedings of the XXIV International Conference on High Energy Physics*, Munich, West Germany, 1987, edited by R. Kotthaus and J. H. Kuhn (Springer, Berlin, 1989), p. 1265; J. F. Gunion, H. E. Haber, G. L. Kane, and S. Dawson, UC Santa Cruz Report No. SCIPP-89/13 (unpublished).
- ⁷V. Barger, T. Han, and R. J. N. Phillips, Phys. Rev. D **37**, 2005 (1988); Phys. Lett. B **206**, 339 (1988).
- ⁸V. Barger and T. Han, Phys. Lett. B **212**, 117 (1988); V. Barger, T. Han, and R. J. N. Phillips, Phys. Rev. D **39**, 146 (1989).
- ⁹A. Tofight-Niaki and J. F. Gunion, Phys. Rev. D **39**, 720 (1989).
- ¹⁰T. G. Rizzo, Phys. Lett. B **217**, 191 (1989).
- ¹¹M. S. Chanowitz and M. K. Gaillard, Phys. Lett. **142B**, 85 (1984); Nucl. Phys. **B261**, 379 (1985); M. Golden and S. Sharpe, *ibid.* **B261**, 217 (1985); M. S. Chanowitz, M. Golden, and H. Georgi, Phys. Rev. Lett. **57**, 2374 (1986); Phys. Rev. D **35**, 1490 (1987).
- ¹²J. C. Pumplin, W. W. Repko, and G. L. Kane, in *Physics of the Superconducting Supercollider, Snowmass, 1986*, proceedings of the Summer Study, Snowmass, Colorado, 1986, edited by R. Donaldson and J. Marx (Division of Particles and Fields of the APS, New York, 1987), p. 211; D. A. Dicus, C. Kao, and W. W. Repko, Phys. Rev. D **36**, 1570 (1987); C. Ahn, M. E. Peskin, B. W. Lynn, and S. Selipsky, Nucl. Phys. **B309**, 221 (1988); K. Hagiwara and H. Murayama, Durham University Report No. DTP/89/24, 1989 (unpublished).
- ¹³H. Baer, V. Barger, D. Karatas, and X. Tata, Phys. Rev. D **36**, 96 (1987); H. Baer *et al.*, Int. J. Mod. Phys. A **2**, 1131, (1987); J. F. Gunion *et al.*, *ibid.* **2**, 1145 (1987); R. M. Barnett *et al.*, in *Experiments, Detectors, and Experimental Areas for the Supercollider* (Ref. 6), p. 178.
- ¹⁴For a review and references to E_6 models, see J. L. Hewett and T. G. Rizzo, Phys. Rep. (to be published).
- ¹⁵T. G. Rizzo and R. W. Robinett, Phys. Lett. B **226**, 117 (1989).
- ¹⁶K. Hagiwara and D. Zeppenfeld, Nucl. Phys. **B274**, 1 (1986).